

# ACKNOWLEDGMENTS

We thank Dr. Paul MacDonald, Byron Glenn, and the Vanderbilt University Reproductive Biology Research Center Tissue Culture Core Laboratory for their assistance.

**Registry No.** LRAT, 117444-03-8; ARAT, 81295-48-9; retinol, 68-26-8; retinyl palmitate, 79-81-2; retinyl stearate, 631-87-8; retinyl oleate, 631-88-9; retinyl linoleate, 631-89-0; retinyl laurate, 1259-24-1; dilaurylphosphatidylcholine, 18285-71-7.

# REFERENCES

- Ahluwalia, B., & Gambhir, K. K. (1976) *Int. J. Vitam. Nutr. Res.* 46, 330.
- Anthony, C. T., & Skinner, M. K. (1989) *Biol. Reprod.* 40, 811.
- Bishop, P. D., & Griswold, M. D. (1987) *Biochemistry* 26, 7511.
- Blaner, W. S., Galdieri, M., & Goodman, D. S. (1987) *Biol. Reprod.* 36, 130.
- Carson, D. D., & Lennarz, W. J. (1983) *J. Biol. Chem.* 258, 1632.
- Chaudhary, L. R., & Nelson, E. C. (1987) *Biochim. Biophys. Acta* 917, 24.
- deRuyter, M. G. M., & de Leenheer, A. P. (1979) *Anal. Chem.* 51, 43.
- Dorrington, J. H., & Fritz, I. B. (1975) *Endocrinology* 96, 879.
- Fawcett, D. W. (1975) in *Handbook of Physiology* (Hamilton, D. W., & Grup, R. D., Eds.) p 21, American Physiological Society, Bethesda, MD.
- Fex, G., & Johannesson, G. (1988) *Biochim. Biophys. Acta* 944, 249.
- Futterman, S., Heller, J. (1972) *J. Biol. Chem.* 247, 5168.
- Karl, A. F., & Griswold, M. D. (1980) *Biochem. J.* 186, 1001.

- Kato, M., Sung, W. K., Kato, K., & Goodman, D. S. (1985) *Biol. Reprod.* 32, 173.
- Liau, G., Ong, D. E., & Chytil, F. (1981) *J. Cell Biol.* 91, 63.
- MacDonald, P. N., & Ong, D. E. (1988a) *J. Biol. Chem.* 263, 12478.
- MacDonald, P. N., & Ong, D. E. (1988b) *Biochem. Biophys. Res. Commun.* 156, 157.
- Ong, D. E., & Chytil, F. (1978) *J. Biol. Chem.* 253, 828.
- Ong, D. E., Kakkad, B., & MacDonald, P. N. (1987) *J. Biol. Chem.* 262, 2729.
- Ong, D. E., MacDonald, P. N., & Gubitosi, A. M. (1988) *J. Biol. Chem.* 263, 5789.
- Ottonello, S., Petrucci, S., & Maraini, G. (1987) *J. Biol. Chem.* 262, 3975.
- Peterson, G. L. (1977) *Anal. Biochem.* 83, 346.
- Porter, S. B., Ong, D. E., Chytil, F., & Orgebin-Crist, M.-C. (1985) *J. Androl.* 6, 197.
- Ritzén, E. M., Hagenas, L., Ploen, L., French, F. S., & Hansson, V. (1977) *Mol. Cell. Endocrinol.* 8, 335.
- Ritzén, E. M., Hansson, V., & French, F. S. (1981) in *The Testis* (Burger, H., & de Kretser, D., Eds.) p 171, Raven Press, New York.
- Saari, J. C., & Bredberg, D. L. (1988) *J. Biol. Chem.* 263, 8084.
- Sanborn, B. M., Steinberger, A., Tcholakian, R. K., & Steinberger, E. (1977) *Steroids* 29, 493.
- Shingleton, J. L., Skinner, M. K., & Ong, D. E. (1989) *Biochemistry* (preceding paper in this issue).
- Skinner, M. K., & Griswold, M. D. (1982) *Biol. Reprod.* 27, 211.
- Tung, P. S., Skinner, M. K., & Fritz, I. B. (1984) *Biol. Reprod.* 30, 199.

## A Differential Scanning Calorimetric Study of the Bovine Lens Crystallins<sup>†</sup>

Bryan L. Steadman,<sup>†</sup> Philip A. Trautman,<sup>‡</sup> Erlinda Q. Lawson,<sup>‡</sup> Matthew J. Raymond,<sup>‡</sup> Deborah A. Mood,<sup>‡</sup> John A. Thomson,<sup>‡</sup> and C. Russell Middaugh<sup>\*,§</sup>

Department of Molecular Biology, University of Wyoming, Box 3944, University Station, Laramie, Wyoming 82071, and Merck Sharp & Dohme Research Laboratories, WP26-331, West Point, Pennsylvania 19486

Received February 9, 1989; Revised Manuscript Received July 31, 1989

**ABSTRACT:** Differential scanning calorimetry was performed on the five major lens crystallin fractions [HM- $\alpha$ ,  $\alpha$ ,  $\beta_H$ ,  $\beta_L$ , and ( $\beta_s + \gamma$ )] of the bovine lens as well as on more purified forms of  $\alpha$ - and  $\gamma$ -crystallins. All were found to be relatively thermally stable although the  $\alpha$ -crystallin fractions were found to at least partially unfold at an approximately 10 °C lower temperature than the  $\beta$  and  $\gamma$  fractions. Increasing protein concentration had little effect on  $\gamma$ -crystallin thermograms but had marked effects on those of the  $\alpha$ - and  $\beta$ -crystallins. Increases in the thermal stability with increasing protein concentration for the  $\beta$ -crystallins can be explained most simply by the known  $\beta_L/\beta_H$  equilibrium, but, in the case of the  $\alpha$ -crystallins, excluded volume effects may be an important factor. In both cases, the increased stability at high concentrations could be of physiological relevance. As well as the expected endothermic unfolding transitions, all of the lens crystallins revealed exothermic peaks that correlate with protein precipitation. Interestingly, this phenomenon occurs only after extensive structural alteration in the case of the  $\alpha$ -crystallins but is present very early in the initial stages of structural perturbation of the  $\beta$ - and  $\gamma$ -crystallins.

**A**lterations in the conformational integrity of the lens crystallins have often been postulated to play a central role

in cataract formation (Harding & Crabbe, 1984). Thus, since there is virtually no protein turnover during the life of a mammalian lens, structural stability would seem an essential functional prerequisite for lens crystallins. The structural stability of a protein is often inferred from spectroscopic measurements, with the protein usually at a relatively low concentration and in the presence of a chemical denaturant.

<sup>†</sup> This work was supported by NIH Grants GM32650, AI00063, and EY06727.

<sup>\*</sup> To whom correspondence should be addressed.

<sup>‡</sup> University of Wyoming.

<sup>§</sup> Merck Sharp & Dohme Research Laboratories.

By contrast, differential scanning calorimetry (DSC) offers a method by which a protein's thermal stability may be examined precisely and directly, over a much broader concentration range, and without the necessity of adding chemical denaturants.

Differential scanning calorimetry directly measures the heat absorbed or liberated by a protein during conformational transitions as a function of temperature. Since light is not involved, DSC avoids the problem of protein photosensitivity, which tends to complicate spectroscopic studies of crystallin stability. The enormous concentration range accessible to DSC also makes this a very attractive method for studying crystallin behavior. It has been convincingly argued that the inherent transparency of the mammalian lens is, in part, a consequence of short-range order between the crystallins (Benedek, 1971; Delaye & Tardieu, 1983) and that the transparency of the cytoplasmic crystallins is greatest at the high protein concentrations ( $\sim 300$ – $600$  mg/mL) encountered in vivo (Delaye & Tardieu, 1983). This concentration range is inaccessible to most other analytical methods. By searching for changes in protein thermal transitions as a function of protein concentration, however, DSC has the potential to identify the existence of any specific intermolecular interactions that might exist between crystallins at their native concentrations. It has previously been demonstrated in a wide variety of different associating protein systems that significant changes in the position and magnitude of DSC transitions are often observed upon changes in the stoichiometry of aggregated macromolecular components (Vickers et al., 1978; Williams et al., 1979; Lysko et al., 1981; Donovan & Elemer, 1985). In contrast, monomeric proteins with no tendency to associate show no change in denaturation temperature or enthalpy up to exceptionally high ( $>600$  mg/mL) protein concentrations (Fujita & Noda, 1981). In this study, we describe the intrinsic thermal stability properties of the major crystallin fractions, and the effect of protein concentration on each of their thermally induced conformational transitions. This initial study has been primarily limited to the more native crystallin "fractions" to enhance its relevance to the in vivo situation.

#### MATERIALS AND METHODS

**Isolation of Lens Crystallins.** Lens crystallins were fractionated by size-exclusion chromatography as described previously (Lawson et al., 1981) except that buffer conditions were altered as indicated. Twenty decapsulated lenses from freshly slaughtered cows (1–2 years old) were thoroughly homogenized in 20 mL of 0.05 M sodium phosphate, 0.1 M sodium chloride, 0.001 M 2-mercaptoethanol, and 0.02% sodium azide, pH 7.0. All DSC experiments were performed in this buffer. After centrifugation at 1500g for 30 min and at 27000g for 1 h, 7–8 mL of supernatant adjusted to  $A_{280\text{nm}} = 100$  was applied to a column of Sepharose CL-6B ( $5 \times 110$  cm) and eluted in the same buffer, at 22 °C. Five well-resolved peaks were obtained and identified as the  $\text{HM}\alpha$ -,  $\alpha$ -,  $\beta_{\text{H}}$ -,  $\beta_{\text{L}}$ -, and  $(\beta_{\text{s}} + \gamma)$ -crystallins by SDS gel electrophoresis and isoelectric focusing in 7 M urea, as described previously (Thomson & Augusteyn, 1985). Following concentration by ultrafiltration, each was rechromatographed on a smaller Sepharose CL-6B column ( $2.5 \times 110$  cm) and concentrated again by ultrafiltration or by a Minicon B15 macrosolute concentrator (Amicon Corp.) to the desired level. Alternatively, final purification was performed with a Pharmacia FPLC system employing a Superose 6 molecular sieve column.

The  $(\beta_{\text{s}} + \gamma)$ -crystallin fraction was in some cases further separated into subfractions  $\gamma\text{I}$ ,  $\beta_{\text{s}}$ ,  $\gamma\text{II}$ ,  $\gamma\text{III}$ , and  $\gamma\text{IV}$  on sulfopropyl (SP)-Sephadex C-50 using a variation of the

method first described by Bjork (1964) and modified by Thomson et al. (1987). The minor fractions  $\gamma\text{I}$  and  $\beta_{\text{s}}$  were not analyzed separately. Fractions III and IV consisted of subfractions  $\text{III}_{\text{a}}$  and  $\text{III}_{\text{b}}$  (approximate ratio 1:2) and  $\text{IV}_{\text{a}}$  and  $\text{IV}_{\text{b}}$  (approximate ratio 3:1), respectively, but no further purification was performed. The  $\gamma\text{II}$  fraction was further purified to remove residual traces of  $\beta_{\text{s}}$  using DEAE-cellulose, a 25 mM ethanolamine buffer (pH 9.5), and a linear 0–0.1 M NaCl salt gradient (Thomson et al., 1987). The final purified  $\gamma\text{II}$  material was found to be  $>99\%$  homogeneous by analytical isoelectric focusing in urea and densitometric scanning (Thomson & Augusteyn, 1985). In addition, a more homogeneous form of  $\alpha$ -crystallin was prepared by isolation of the  $\alpha\text{A}_2$  chain by ion-exchange chromatography on DEAE-cellulose in the presence of 6 M urea (van Kleef et al., 1974). A form of  $\alpha$ -crystallin which we will refer to as  $\alpha_{\text{r}}(\text{A}_2)$ -crystallin (Thomson, 1985) was then prepared by reassembly of the  $\alpha\text{A}_2$  chains by removal of the urea by dialysis (Thomson et al., 1985). The resulting  $\alpha_{\text{r}}(\text{A}_2)$  was found to be homogeneous by both analytical isoelectric focusing in urea and quasi-elastic light scattering.

**Differential Scanning Calorimetry.** Calorimetry experiments were carried out with either a Microcal MC-1 or a Hart 7708 differential scanning calorimeter. Protein concentrations were determined spectrophotometrically (Lawson et al., 1981), after vacuum degassing of samples immediately prior to being loaded into the calorimeter cells. A scan rate of 60 °C/h was generally employed, although rates were occasionally varied from 40 to 80 °C/h. Only small differences were seen over this limited range of scanning rates. Actual tracings of representative scans are shown in Figures 1–6 and have been offset for clarity (except Figure 6). All of the data in the figures are from the Hart instrument and are expressed on a weight basis. Each protein concentration was examined a minimum of 5 times using different sample preparations for each experiment. Reproducibility of transition temperatures was found to be on the order of 0.5–1 °C, and absolute intensities of heat capacity changes varied by 3–5%. Reversibility was tested by returning previously scanned solutions to 10 °C, incubating for times ranging from several minutes to overnight and rescanning the solutions.

**Miscellaneous Methods.** Turbidity measurements were performed under temperature scanning conditions identical with those employed in the differential scanning calorimetry experiments. Turbidity was monitored continuously at 350 nm employing a Hitachi 100-8 spectrophotometer. Temperature was controlled with a Neslab RTE-50D refrigerated circulating water bath, and sample temperature was varied at a rate of 60 °C/h with a Neslab MTP-5 programmer. Measurements of  $\text{OD}_{350\text{nm}}$  versus temperature were performed over the same range of protein concentrations used in the DSC experiments for each of the crystallin fractions.

Fluorescence emission from tryptophan residues (excitation at 295 nm) was determined with an SLM 4000 spectrofluorometer between 350 and 300 nm. Circular dichroism was measured from 250 to 200 nm with a Jasco J500A spectropolarimeter. Temperature was varied in both cases with a circulating water bath, and samples were equilibrated for 15 min prior to each measurement. A protein concentration of 0.05 mg/mL was used in both fluorescence and CD studies to reduce interference from light scattering.

#### RESULTS

In a differential scanning calorimetric experiment, a disruption of native, macromolecular structure is usually accompanied by an endothermic (positive) transition in the

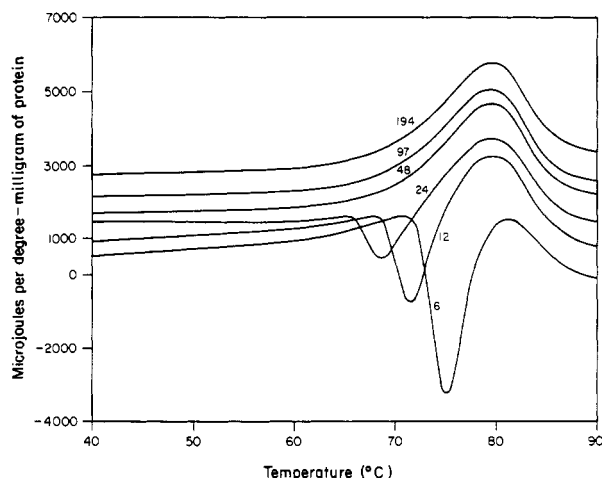


FIGURE 1: Tracings of typical differential scanning calorimeter thermograms (heat capacity versus temperature) of unfractionated bovine lens  $\gamma$ -crystallin. The numbers next to each scan are the protein concentrations in milligrams per milliliter. All experiments were performed in a buffer containing 0.05 M sodium phosphate, 0.1 M sodium chloride, 0.001 M 3-mercaptoethanol, and 0.02% sodium azide, pH 7.0, and at a scanning rate of 60  $^{\circ}\text{C}/\text{h}$ .

thermogram (Privalov, 1979, 1982). In contrast, when new interactions occur such as in an aggregation process, an exotherm is usually observed.

Representative thermograms of  $(\beta_s + \gamma)$ -crystallin (isolated by size exclusion) over a wide range of protein concentration are illustrated in Figure 1. At higher protein concentrations, a broad endothermic transition is apparent centered near 80  $^{\circ}\text{C}$ , consistent with previous observations by others (Zhang et al., 1986). As protein concentration is lowered, an exotherm begins to appear in front of the endothermic transition. This exotherm increases in intensity and shifts to higher temperature as protein concentration decreases until it partially obscures the endothermic peak. Within the limits of resolution imposed by the exotherm, the endothermic transition appears to be independent of protein concentration over the range of protein concentration (6–194 mg/mL) examined. A careful examination of the higher protein concentrations in Figure 1 shows the endothermic transition to be slightly asymmetric with the leading edge more gradual in slope. The  $\gamma$ -crystallin examined in these studies is heterogeneous, consisting of a mixture of at least six major polypeptides.

To explore the potential role of heterogeneity in the shape of the endothermic transition, the  $(\beta_s + \gamma)$ -crystallin fraction was further fractionated into its  $\gamma\text{II}$ ,  $\gamma\text{III}$ , and  $\gamma\text{IV}$  components and examined at higher protein concentrations where no interference from exotherms was observable. Both  $\gamma$ -crystallin fractions III and IV contain at least two components as shown by further fractionation (Bjork, 1964). As seen in Figure 2, they also manifest pronounced shoulders on the leading edges of their thermograms. In contrast, the  $\gamma\text{II}$ -crystallin fraction, which was further purified to an apparently homogeneous state, showed no shoulder in the same area of its thermogram. However, the asymmetry of the front limb, in the crude  $\gamma$ -crystallin fraction, is still apparent.

Thermograms from the low molecular weight fraction of  $\beta$ -crystallin are shown over a protein concentration range of 3–110 mg/mL in Figure 3. Both endo- and exotherms are observed for each concentration, although the endotherm is obscured by the strong exotherm seen at the lowest concentration. As seen with the  $\gamma$ -crystallins, the exotherm becomes more pronounced and shifts to higher temperature as protein concentration decreases. In contrast, the endotherm shifts to

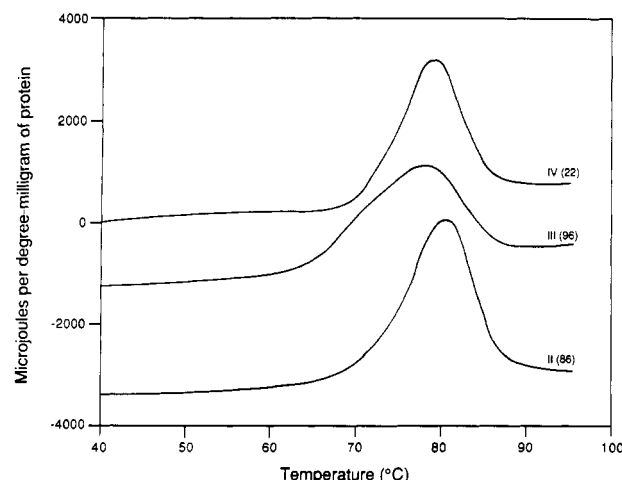


FIGURE 2: DSC thermograms of the three major bovine  $\gamma$ -crystallin subfractions (see Materials and Methods for description of each fraction). Conditions are the same as those in Figure 1 with protein concentrations given in parentheses next to the roman numerals identifying each  $\gamma$ -crystallin type.

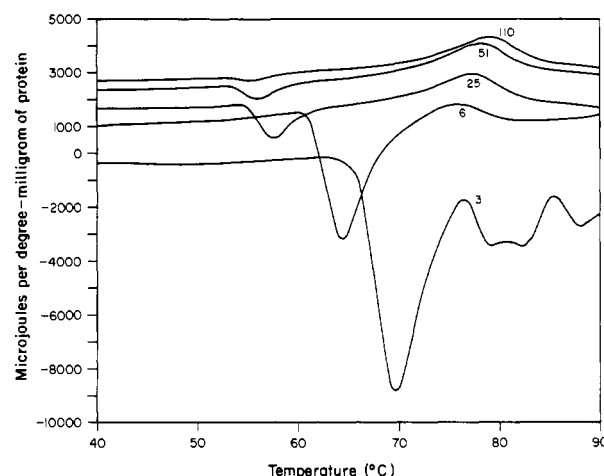


FIGURE 3: DSC thermograms of the low molecular weight form of  $\beta$ -crystallin at indicated varying protein concentrations. Experimental conditions are the same as those in Figure 1.

higher temperature (76  $\rightarrow$  80  $^{\circ}\text{C}$ ) as the protein concentration is raised. This endotherm also differs from that seen with  $\gamma$ -crystallin in that it displays both marked leading and trailing tails.

The higher molecular weight form of  $\beta$ -crystallin displays somewhat different behavior. At lower concentrations, an exotherm is again present. Its position appears to be independent of protein concentration, but its relative magnitude decreases with increasing protein concentration until it is no longer detectable at the highest concentration examined (Figure 4). The endotherm near 80  $^{\circ}\text{C}$  displays a small concentration dependence, shifting to higher temperature at higher protein concentration by perhaps 1–2  $^{\circ}\text{C}$ . As protein concentration is lowered, very distinct shoulders become increasingly noticeable on the main endothermic transition.

The  $\alpha$ -crystallin fraction (Figure 5) manifests a protein concentration independent endothermic transition centered near 70  $^{\circ}\text{C}$ . This endotherm also contains a significant shoulder 6–10  $^{\circ}\text{C}$  above the main endotherm which increases in intensity with increasing protein concentration. As protein concentration is lowered, an exotherm begins to appear on the high-temperature side of the endothermic transition. Because of the intrinsic heterogeneity of the  $\alpha$ -crystallin fraction and the fact that the protein consists of two distinct types of po-

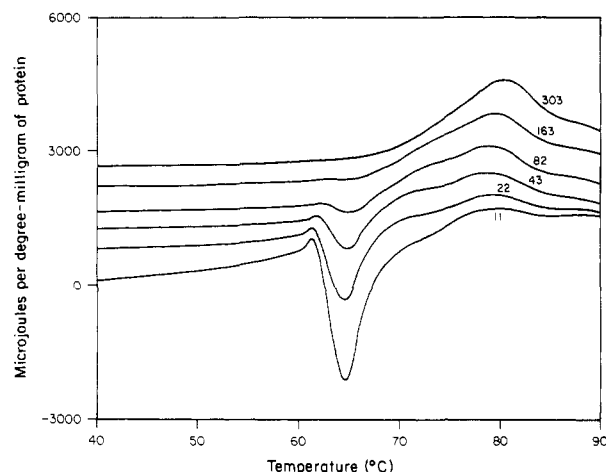


FIGURE 4: DSC thermograms at various protein concentrations of the high molecular weight fraction of bovine  $\beta$ -crystallin. Experimental conditions are identical with those employed in Figure 1.

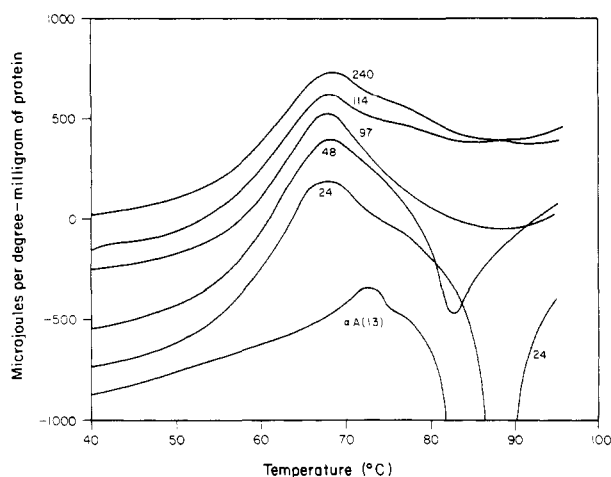


FIGURE 5: DSC thermograms at varying protein concentration of bovine  $\alpha$ -crystallin. The lowest trace is of a form of  $\alpha$ -crystallin at 13 mg/mL produced by the reassembly of purified  $\alpha_2$  chains. Conditions are again as described in Figure 1.

lypeptide chains (A and B), we reassembled a more homogeneous form of  $\alpha$ -crystallin,  $\alpha_r(A_2)$ , by reassociation of pure  $\alpha_2$  chains. As shown in Figure 5, the  $\alpha_r(A_2)$  produces an endothermic transition shifted to several degrees higher temperature. Although the usual exothermic transition seen at lower protein concentration partially hides the main endotherm, evidence for complexity in the endotherm is still apparent in the form of both high- and low-temperature shoulders.

The high molecular weight form of  $\alpha$ -crystallin produces a very broad endothermic transition with evidence for two components (Figure 6) near 65 and 77 °C. The magnitude of these transitions is dependent on protein concentration, going through a maximum somewhere between 8 and 35 mg/mL. The thermograms in Figure 6 have not been displaced to emphasize this point. It is interesting to note that the endothermic transitions are initiated at a very low temperature (40 °C) relative to the other crystallins. The complex endotherm is again followed by a strong exothermic transition which decreases in intensity and temperature of occurrence as protein concentration is raised.

Reversibility of DSC transitions for each protein at both high and low protein concentration was monitored by returning scanned material to various temperatures prior to transition regions, incubating for various lengths of time, and rescanning.

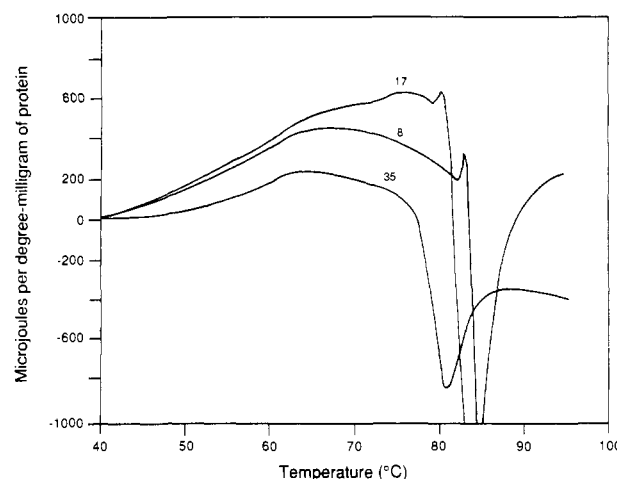


FIGURE 6: DSC thermograms at three different protein concentrations of the high molecular weight fraction of bovine  $\alpha$ -crystallin (conditions as in Figure 1).

In the neutral buffer solutions employed in these experiments, at best only partial reversibility could be observed for the two  $\alpha$ -crystallin fractions. No reversibility for the  $\beta$ - and  $\gamma$ -crystallins could be detected under these conditions.

In an attempt to confirm the origin of the exothermic and endothermic transitions seen in the thermograms, several additional experiments were performed. Light scattering from each of the five crystallin fractions was monitored by turbidity measurements as solution temperature was raised at the same rate employed in the DSC studies. Turbidity changes occurring at a rate of 60 °C/h at a protein concentration of 2 mg/mL are illustrated in Figure 7C. It is seen that significant light scattering began to appear several degrees prior to DSC exothermic transitions. At higher protein concentrations, where no exotherms are detectable, light scattering is also observed, but its magnitude is significantly less on a protein weight basis than that observed at lower concentrations.

To examine the onset of temperature-induced protein conformational changes, equilibrium temperature dependent spectral studies were performed at low protein concentrations (0.05 mg/mL) using circular dichroism measurements at 217 nm (Figure 7B) and fluorescence intensity at the peak maximum for each protein (Figure 7A). The CD results showed a large temperature-dependent loss of intensity at ellipticity minima consistent with a significant change in secondary structure for all proteins. The HMW form of  $\alpha$ -crystallin appears to partially maintain some secondary structure at high temperature, manifesting only a small change in the ellipticity minimum at 217 nm (Maiti et al., 1988). Therefore, the ellipticity at 205 nm is shown in Figure 7B for this protein to emphasize the formation of disordered structure. These changes occurred over the temperature ranges of the corresponding DSC endotherms although the more sensitive spectral measurements reveal changes prior to the DSC alterations. Analogous abrupt increases in both fluorescence intensity (not illustrated) and emission peak maxima are also observed in the region of the corresponding DSC endotherms for each crystallin fraction.

The DSC transitions observed in this study were completely irreversible at pH 7.0 with the exception of the  $\alpha$ -crystallins which manifest partial reversibility. Irreversibility prevents the direct calculation of heats of denaturation from areas under the transition curves, or heat capacity changes from base-line alterations. Sturtevant has shown, however, that if linear van't Hoff plots of DSC data (logarithm of protein concentration versus reciprocal transition temperature) can be obtained for

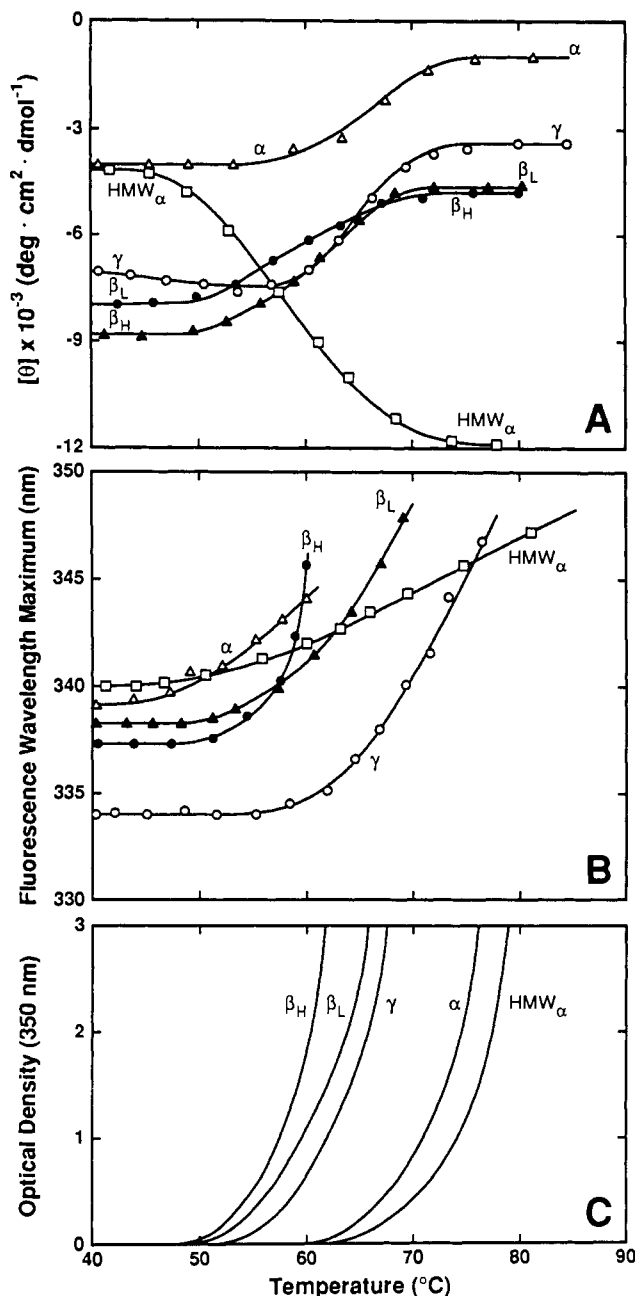


FIGURE 7: (A) Effect of temperature on the circular dichroism of the five major lens crystallin fractions. The ellipticity at 217 nm is shown as a function of temperature under equilibrium conditions. In the case of the  $\text{HMW}_\alpha$  fraction, the value of  $[\theta]$  at 205 nm is actually shown to enhance the spectral differences. All measurements were performed in the same phosphate buffer used in the DSC experiments at a protein concentration of 0.05 mg/mL in 1-mm path-length cells. (B) Effect of temperature on the fluorescence maximum of the five crystallin fractions employing excitation at 295 nm. Solution conditions were the same as those in (A). (C) Turbidity recorded continuously as a function of temperature at a rate of change of temperature of 60 °C/h. The experiments shown were performed at a protein concentration of 2 mg/mL employing 1-cm path-length cells in the same experimental phosphate buffer.

oligomeric proteins, the identity of van't Hoff and calorimetric enthalpies can be used as criteria for the calculation of true heats of transition (Takahashi & Sturtevant, 1981; Edge et al., 1985). We have attempted such an analysis for the  $\alpha$ - and  $\beta$ -crystallins. For several reasons, this has been unsuccessful. First, in many cases, we have been unable to uniquely deconvolute the multiple transition containing thermograms by various nonlinear least-squares methods because of the low signal to noise ratio of much of the data at lower protein

concentrations and extensive peak overlap. The positions of the deconvoluted transitions are very sensitive to the nature of the deconvolution process, introducing significant uncertainty into the analysis. In fact, in many cases, the van't Hoff plots are nonlinear. In others, infinite slopes are encountered (i.e., no temperature dependence of peak position on protein concentration). In still other instances where linear van't Hoff plots are encountered, the values of the calorimetric and van't Hoff enthalpies are not in agreement, presumably due to the multistate nature of the thermal unfolding process (Privalov, 1982). Finally, interference from exothermic transitions complicates most of the data at lower protein concentrations. For these reasons, we will not present any quantitative thermodynamic analysis of the DSC crystallin data, but rather will focus on more qualitative features of the thermograms.

## DISCUSSION

As a group, the lens crystallins appear to be relatively thermally stable proteins, all manifesting large endothermic transitions between 60 and 90 °C. Each of the five crystallins exhibit large red shifts in their intrinsic tryptophan fluorescence maxima and alterations in ultraviolet circular dichroism ellipticity minima in the same temperature range as the DSC endothermic transitions. Although these results are complicated by light scattering and the lower concentrations at which they were obtained, they are consistent with extensive protein unfolding during the endothermic events. Similar changes have been detected by others using a variety of techniques (Maiti et al., 1988; Zhang et al., 1986).

The origin of the exothermic transitions seen at lower protein concentrations with all of the proteins seems to be due to fairly extensive protein aggregation. This is most directly demonstrated by the onset of significant light scattering just prior to the appearance of the transitions (Figure 7C). The disappearance of the exotherms at higher protein concentration may be partially due to the fact that the heat of precipitation involves proportionally less of the total heats when large amounts of protein are present. More significantly, it appears that convection effects arising from thermally induced motion of the precipitated material make a contribution to the exotherms. This is supported by the fact that when small capillaries are inserted into the calorimetry cell to reduce the formation of large particles, the magnitude of the exotherms is dramatically reduced (not illustrated). In addition, some inhibition of precipitation may be occurring, although precipitation itself is still detectable by light scattering at high protein concentrations. Interestingly, this precipitation appears at the very beginning of the endothermic (protein unfolding) transitions in the case of the  $\gamma$ - and  $\beta$ -crystallins while it only occurs after substantial protein unfolding with the  $\alpha$  fractions. It thus appears that only rather subtle structural alterations are necessary to produce that aggregation of the  $\gamma$ - and  $\beta$ -crystallins, while the  $\alpha$ -crystallins only show such behavior after more extensive protein unfolding. Since cataract formation may sometimes involve crystallin conformational changes and subsequent aggregation (Harding & Crabbe, 1984), these intrinsic differences in aggregation properties of the various crystallins may be important in understanding related pathological processes.

Several interesting observations can be made on the basis of the concentration dependence of the crystallin DSC transitions. In the case of the  $\gamma$ -crystallins, little or no concentration dependence is detected. Thus, at least for these monomeric proteins in homogeneous protein solution there is no evidence for stabilization by aggregation at high protein concentration. Despite this observation, there is evidence for

aggregation of at least some  $\gamma$ -crystallins at the higher protein concentrations used in the DSC experiments (Siezen et al., 1985).

In contrast, both the  $\beta$  and  $\alpha$  fractions show significant protein concentration dependence in their thermograms. A partial explanation for the concentration dependence of the  $\beta_L$  and  $\beta_H$  fractions can be offered in terms of the previously described dimer-hexamer equilibrium between the two forms (Bindels et al., 1981; Siezen et al., 1986). When  $\beta_L$ -crystallins are concentrated to above about 50 mg/mL, their thermograms display primarily a single high-temperature transition, characteristic of the hexameric  $\beta_H$  form. The thermograms gradually begin to manifest a second, lower temperature transition as protein concentration is lowered, which may correspond to the dimeric form. In an analogous fashion, the  $\beta_L$  exotherm seen at lower protein concentration begins to shift to higher temperature as protein concentration is raised, consistent with a shift to the hexameric ( $\beta_H$ ) form. It should be noted that the calorimetric changes shown in this study occur over the same concentration range as the chromatographic changes previously reported in the characterization of the  $\beta$ -associative properties (Siezen et al., 1986). The data in Figures 3 and 4 can thus be simply accounted for by the  $\beta_L/\beta_H$  equilibrium. Thus, increasing protein concentration leads to increasing stability of the  $\beta$ -crystallins, possibly a physiologically desirable situation. The structural complexity of the two  $\beta$ -crystallin fractions, however, precludes more definitive conclusions.

As the protein concentration of low molecular weight  $\alpha$ -crystallin is raised, evidence for a more thermally stable form is also clearly evident. Previous evidence for only very limited aggregation of  $\alpha$ -crystallin at high concentrations has been found on the basis of dynamic light-scattering measurements (Andries & Clauwaert, 1985), suggesting that increased self-association may not be responsible for the observed changes. Preliminary dynamic light-scattering results from our laboratory indicate that observable large aggregates in  $\alpha$ -crystallin solutions at high concentrations comprise only a fraction of a percent of the total (Trautman and Middaugh, unpublished results). This small amount of aggregated material would not be expected to contribute significantly to the observed thermogram. A simple alternative explanation for stabilizing effects can be offered in terms of excluded volume phenomena. If the "macromolecular crowding" produced at high protein concentrations preferentially stabilizes either the folded or the unfolded form of the protein, then a perturbation of protein stability would result (Zimmerman & Harrison, 1987). Previous reports of complete thermal stability of  $\alpha$ -crystallin up to 100 °C (Maiti et al., 1988) are not supported by this work. Inspection of Figure 1 from this previous work, however, does show evidence for a thermal event at the same temperature found in the present work.

The results with the high molecular weight form of  $\alpha$ -crystallin (HM- $\alpha$ ) are less clear due to the presence of the exothermic transition at all accessible concentrations, although the presence of a peak in the region of the less aggregated form is clearly evident. The effect of high protein concentration is again a stabilizing one.

Differential scanning calorimetry also offers the possibility of probing the existence of structural domains within polypeptide chains. The equilibria discussed above currently prohibit rigorous consideration of this possibility for the  $\alpha$  and

$\beta$  fractions, but studies of the more purified monomeric  $\gamma$ -crystallins suggest the existence of such domains as previously shown in the X-ray structure of bovine  $\gamma$ II-crystallin (Wistow et al., 1983). The lack of symmetry in the denaturation endotherm of pure  $\gamma$ II-crystallin can most simply be accounted for by this dual domain structure. In support of this, in preliminary experiments at low pH, we have been able to completely resolve two distinct transitions in preparations of  $\gamma$ -crystallin (unpublished results) as well as obtain partial reversibility. Thus, we are presently investigating the use of DSC to obtain a complete thermodynamic analysis of the individual  $\gamma$ -crystallins under selected solution conditions.

## REFERENCES

- Andries, C., & Clauwaert, J. (1985) *Biophys. J.* **47**, 591–605.
- Benedek, G. (1971) *Appl. Opt.* **10**, 459–473.
- Bindels, J. G., Koppers, A., & Hoenders, H. J. (1981) *Exp. Eye Res.* **33**, 333–343.
- Bjork, I. (1964) *Exp. Eye Res.* **3**, 254–261.
- Delage, M., & Tardieu, A. (1983) *Nature* **302**, 415–417.
- Donovan, J. W., & Mihalyi, E. (1985) *Biochemistry* **24**, 3434–3443.
- Edge, V., Allewell, N. M., & Sturtevant, J. M. (1985) *Biochemistry* **24**, 5899–5906.
- Fujita, Y., & Noda, Y. (1981) *Int. J. Pept. Protein Res.* **18**, 12–17.
- Harding, J. J., & Crabbe, J. C. (1984) in *The Eye* (Davson, H., Ed.) 3rd ed., Vol. IB, pp 207–492, Academic Press, New York.
- Lawson, E. Q., Schubert, C. F., Lewis, R. V., & Middaugh, C. R. (1981) *J. Biol. Chem.* **256**, 6523–6525.
- Lysko, K. A., Carlson, R., Taverna, R., Snow, J., & Brandts, J. F. (1981) *Biochemistry* **20**, 5570–5576.
- Maiti, M., Kono, M., & Chakrabarti, B. (1988) *FEBS Lett.* **236**, 109–114.
- Privalov, P. L. (1979) *Adv. Protein Chem.* **33**, 167–241.
- Privalov, P. L. (1982) *Adv. Protein Chem.* **35**, 1–104.
- Siezen, R. J., Fisch, M. R., Slingsby, C., & Benedek, G. B. (1985) *Proc. Natl. Acad. Sci. U.S.A.* **82**, 1701–1705.
- Siezen, R. J., Anello, R. D., & Thomson, J. A. (1986) *Exp. Eye Res.* **43**, 293–303.
- Takahashi, K., & Sturtevant, J. M. (1981) *Biochemistry* **20**, 6185–6190.
- Thomson, J. A. (1985) Ph.D. Thesis, University of Melbourne, Melbourne, Australia.
- Thomson, J. A., & Augusteyn, R. C. (1985) *Exp. Eye Res.* **40**, 393–410.
- Thomson, J. A., Hum, T. P., & Augusteyn, R. C. (1985) *Aust. J. Exp. Biol. Med. Sci.* **63**, 563–571.
- van Kleef, F. S. M., Nijzink-Maas, M. J. C. M., & Hoenders, H. J. (1974) *Eur. J. Biochem.* **48**, 563–570.
- Vickers, L. P., Donovan, J. W., & Schachman, H. K. (1978) *J. Biol. Chem.* **253**, 8493–8498.
- Williams, K. R., Sillerud, L. O., Schafer, D. E., & Konigsberg, W. H. (1979) *J. Biol. Chem.* **254**, 6426–6432.
- Wistow, G., Turnell, B., Summers, L., Slingsby, C., Moss, D., Miller, L., Lindley, P., & Blundell, T. (1983) *J. Mol. Biol.* **170**, 175–202.
- Zhang, J. Z., Zhang, Z. L., Zhang, Y. Z., Li, R. W., & Wolanczyk, J. P. (1986) *Top. Aging Res. Eur.* **6**, 223–226.
- Zimmerman, S. B., & Harrison, B. (1987) *Proc. Natl. Acad. Sci. U.S.A.* **84**, 1871–1875.